

Temperature Induced Hydrophobic Adsorption and Desorption of Linear Polymer Chains on Surfactant-Free Latex Nanoparticles

Tengjiao Hu,[†] Jun Gao,[‡] and Chi Wu^{*,†,‡}

The Open Laboratory of Bond-selective Chemistry, Department of Chemical Physics, University of Science and Technology of China, Hefei, Anhui, 230026 China, and Department of Chemistry, The Chinese University of Hong Kong, Shatin, N. T., Hong Kong

Helmut Auweter and Ruediger Iden

Department of Solid State Physics & Polymer Physics, BASF AG, Ludwigshafen, Rhine, Germany

Received: October 2, 2001; In Final Form: June 3, 2002

The adsorption of thermally sensitive poly(*N*-isopropylacrylamide) (PNIPAM) on surfactant-free polystyrene latex was used as a model system to study the effect of chain hydrophobicity on the adsorption of protein on hydrophobic surface. PNIPAM is only soluble in water at lower temperatures with a lower critical solution temperature (LCST) of ~ 32 °C. Using PNIPAM, we were able to continuously adjust the chain hydrophobicity and manipulate the adsorption by a simply temperature variation. A combination of static and dynamic laser light scattering was used to study the amount of the adsorption and the thickness of the adsorbed polymer layer. We found that there existed a hysteresis of the adsorption in the heating-and-cooling cycle, indicating an additional adsorption at temperatures higher than the LCST. We also found that the heating rate could greatly affect the adsorption. Our results revealed that the desorption accompanying the swelling of the adsorbed PNIPAM layer was logarithmically proportional to the desorption time, indicating a diffusion-controlled process.

Introduction

The adsorption of polymer chains on surfaces is not only an interesting scientific problem, but also has many important industrial applications.^{1–3} Most of the past studies have focused on the conformation and mobility of the adsorbed polymer chains. It has been generally known that the conformation of a long polymer chain adsorbed on a surface is in the form of a “train”, “loop”, or “tail”. A “train” represents the adsorption of most of the monomers of a segment of the chain on the surface, a “loop” is formed via the adsorption of the first and the last monomer units of the segment on the surface, and a “tail” is the free end of the chain. A spin-labeling experiment showed two rotational correlation times, corresponding to the slow motion of the “train” and the fast motion of the “loop” or “tail”.⁴ To study adsorption, colloidal particles are often used as a model substrate.⁵ Using narrowly distributed polymeric latex particles can simplify the problem and lead to a better understanding of adsorption. Recently, the adsorption of proteins on polymeric particles has attracted much attention because of its biomedical applications.^{6,7} However, proteins are very complicated macromolecules and their adsorption involves both electrostatic and hydrophobic interactions. It is normally difficult to separate them in an adsorption experiment.

To attack the problem step by step, we used a neutral protein-like homopolymer, poly(*N*-isopropylacrylamide) (PNIPAM), to study the adsorption and desorption of polymer chains on a particle surface. PNIPAM as a thermally sensitive polymer has been extensively studied.⁸ It is hydrophilic and water soluble

at lower temperatures with a lower critical solution temperature (LCST) of ~ 32 °C.⁹ Kawaguchi et al.¹⁰ investigated the adsorption of PNIPAM chains on silicon surfaces and found that adsorption was enhanced by increasing hydrophobic interaction. Our previous results showed that adsorption increased with PNIPAM concentration and incubation temperature.¹¹

On the other hand, it is generally known that desorption is influenced by topological constraints and thermodynamics.¹² The desorption of a long polymer chain from a surface is an extremely slow process.¹³ It is our intention in this study to address the hydrophobicity dependence of the adsorption and desorption of polymer chains onto a hydrophobic surface. Using PNIPAM enables us to change the chain hydrophobicity and manipulate the adsorption by a temperature variation.⁹ Moreover, the surfactant-free monodispersed polystyrene nanoparticles used as a substrate in this study were much smaller than those previously used, so the adsorption and desorption could lead to a larger change in size and mass of the particles, making the results more precise and reliable.

Experimental Section

Sample Preparation. Two narrowly distributed surfactant-free polystyrene latex dispersions ($\langle R_h \rangle = 22$ and 60 nm, respectively denoted as PS22 and PS60) and four PNIPAM samples ($M_w = 7.0 \times 10^3$, 8.6×10^4 , 8.4×10^5 , and 6.0×10^6 g/mol, respectively denoted as PN1, PN2, PN3, and PN4) were used. The synthesis and fractionation of PNIPAM were detailed before.¹⁴ The hydrodynamic radii of the PNIPAM chains in water at 25 °C were ca. 3, 10, 34, and 110 nm, respectively. The adsorption saturation at room temperature could be reached within minutes after mixing the PNIPAM solution with the

* Address correspondence to this author at The Chinese University of Hong Kong.

[†] University of Science and Technology of China.

[‡] The Chinese University of Hong Kong.

nanoparticle dispersion. The final latex concentration was kept at 1.0×10^{-5} g/mL. Doubly distilled deionized water was used as the dispersant. The resultant dispersions were clarified using a 0.5- μ m filter to remove dust.

Laser Light Scattering. The detail of the laser light scattering (LLS) instrumentation can be found elsewhere.^{15,16} The specific refractive index increment (dn/dC) was determined by using a novel and precise differential refractometer.¹⁷ In static LLS, the angular dependence of the absolute excess time-averaged scattered intensity $R_{vv}(\theta)$, known as the Rayleigh ratio, was measured. For a very dilute solution, the weight average molar mass (M_w) is related to $R_{vv}(\theta)$ by¹⁸

$$\frac{K'(dn/dC)^2 C}{R_{vv}(q)} \cong \frac{1}{M_w} \left(1 + \frac{1}{3} \langle R_g^2 \rangle_z q^2 \right) \quad (1)$$

where $K' = 4\pi^2 n^2 / (N_{Av} \lambda_o^4)$ and $q = (4\pi n / \lambda_o) \sin(\theta/2)$ with N_{Av} , n , and λ_o being the Avogadro constant, the solvent refractive index, and the laser wavelength in a vacuum, respectively; $\langle R_g^2 \rangle_z^{1/2}$ (or simply $\langle R_g \rangle$) is the z -average root-mean-square radius of gyration. In this study, the mixture was so diluted that the extrapolation of $[R_{vv}(\theta)]_{C \rightarrow 0}$ was not necessary. Note that the light scattered from each nanoparticle was so strong that the intensities of the light scattered from water and individual nonadsorbed PNIPAM chains free in water could be neglected. For adsorption, it is reasonable to consider the particle adsorbed with PNIPAM as a polymeric core-shell nanostructure. We were able to use a simple weight additive method to calculate dn/dC ,¹⁹ i.e.

$$\left(\frac{dn}{dC} \right)_{PS+PNIPAM} = \chi_{PNIPAM} \left(\frac{dn}{dC} \right)_{PNIPAM} + (1 - \chi_{PNIPAM}) \left(\frac{dn}{dC} \right)_{PS} \quad (2)$$

where $\chi_{PNIPAM} = \gamma W_{PNIPAM} / (\gamma W_{PNIPAM} + W_{PS})$ with W_{PS} and W_{PNIPAM} being the macroscopic weights of the particles and PNIPAM, respectively; and γ being the fraction of the PNIPAM chains adsorbed on the particles. Therefore, the weight concentration (C) of the particles adsorbed with PNIPAM is $(W_{PS} + \gamma W_{PNIPAM})/V$, or $(1 + \gamma W_{PNIPAM}/W_{PS})C_{PS}$, where $C_{PS} [= W_{PS}/V]$ is the initial particle concentration before the adsorption.

The measured specific refractive index increments of the PNIPAM chains and the particles in water at $\lambda = 488$ nm are 0.167 and 0.256 mL/g, respectively. A combination of eqs 1 and 2 leads to

$$(M_w)_{PS+PNIPAM} = \frac{[R_{vv}(q \rightarrow 0)]_{PS+PNIPAM}}{K[(dn/dC)_{PS+PNIPAM}^2] C_{PS+PNIPAM}} \quad (3)$$

where $[R_{vv}(q \rightarrow 0)]_{PS+PNIPAM}$ and $(M_w)_{PS+PNIPAM} [= (1 + \gamma W_{PNIPAM}/W_{PS})(M_w)_{PS}]$ are the Rayleigh ratio and the weight-average molar mass of the particles after adsorption, respectively, and $(M_w)_{PS} [= [R_{vv}(q \rightarrow 0)]_{PS} / \{ (K' (dn/dC)_{PS}^2 C_{PS}) \}]$ is the weight-average molar mass of the particles before adsorption. Equation 3 can be rearranged as

$$\gamma \frac{W_{PNIPAM}}{W_{PS}} = \frac{(dn/dC)_{PS}}{(dn/dC)_{PNIPAM}} \left\{ \left(\frac{[R_{vv}(\theta \rightarrow 0)]_{PS+PNIPAM}}{[R_{vv}(\theta \rightarrow 0)]_{PS}} \right)^{1/2} - 1 \right\} \quad (4)$$

where $[R_{vv}(\theta \rightarrow 0)]_{PS}$ is a constant for a given C_{PS} , dn/dC can be independently measured, and W_{PNIPAM}/W_{PS} is a known parameter from the sample preparation, so that γ can be

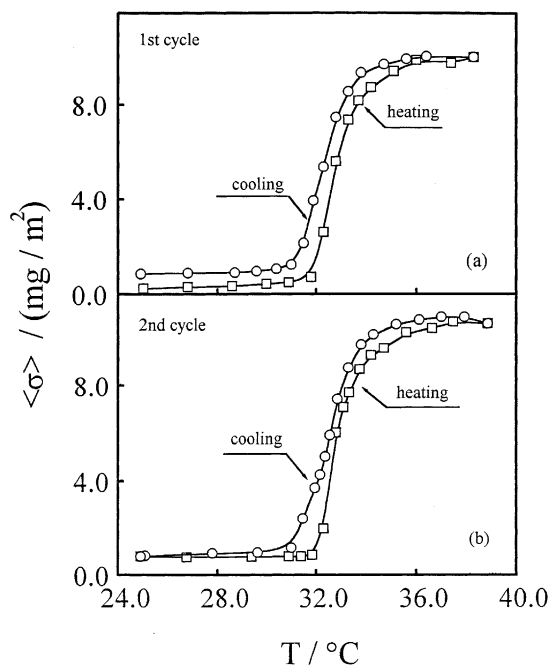


Figure 1. Temperature dependence of adsorption density ($\langle \sigma \rangle$) for the mixture of PN2 and PS22. $\langle \sigma \rangle = (M_w - M_{w,o}) / [4\pi \langle R_{h,o} \rangle^2]$; $M_{w,o}$ and M_w are the weight-average molar masses of the particles before and after adsorption, respectively, $\langle R_{h,o} \rangle$ is the average hydrodynamic radius of the particle before adsorption, and the PN2/PS22 macroscopic weight ratio is 2.

determined from $[R_{vv}(\theta \rightarrow 0)]_{PS+PNIPAM}$ measured in static LLS. It should be noted that $\gamma W_{PNIPAM}/W_{PS}$ represents the weight ratio of the adsorbed PNIPAM chains to the particles. Knowing the average mass and size of each particle, we are able to convert $\gamma W_{PNIPAM}/W_{PS}$ to the average mass of the adsorbed PNIPAM chains ($\langle m \rangle$) per particle or the adsorption density ($\langle \sigma \rangle$) defined as $\langle \sigma \rangle = \langle m \rangle / (4\pi \langle R_{h,o} \rangle^2)$, where $\langle R_{h,o} \rangle$ is the average hydrodynamic radius of the particles before adsorption.

In dynamic LLS, the cumulant analysis of the measured intensity-intensity time correlation function $G^{(2)}(\tau, \theta)$ in the self-beating mode could result in an average line width $\langle \Gamma \rangle$. For a diffusive relaxation, $(\langle \Gamma \rangle / q^2)_{C \rightarrow 0, q \rightarrow 0}$ leads to the average translational diffusion coefficient $\langle D \rangle$ or further to the averaged hydrodynamic radius $\langle R_h \rangle (= k_B T / 6\pi \eta \langle D \rangle)$, where k_B , T , and η are the Boltzmann constant, absolute temperature, and solvent viscosity, respectively. The hydrodynamic volume (V) of the PNIPAM layer adsorbed on the particle surface is related to the radius difference (ΔR_h) between the particle after and before adsorption by²⁰

$$V = (4/3)\pi [(\langle R_h \rangle + \Delta R_h)^3 - \langle R_h \rangle^3] = (4/3)\pi \langle R_{h,o} \rangle^3 f(\Delta R_h / \langle R_{h,o} \rangle) \quad (5)$$

where $f(\Delta R_h / \langle R_{h,o} \rangle) = 3(\Delta R_h / \langle R_{h,o} \rangle) + 3(\Delta R_h / \langle R_{h,o} \rangle)^2 + (\Delta R_h / \langle R_{h,o} \rangle)^3$. It can be seen that using small nanoparticles enabled us to accurately determine ΔR_h and V .

Results and Discussion

Figure 1 shows that when the temperature is higher than the LCST ($\sim 32^{\circ}\text{C}$), there exists an expected sharp increase of the adsorption. This is because PNIPAM becomes hydrophobic and participates on the particle surface at higher temperatures. The adsorption approaches a constant when $T > 35^{\circ}\text{C}$. The adsorption density $\langle \sigma \rangle$ was calculated from the average mass of PNIPAM adsorbed on each nanoparticle as discussed before.

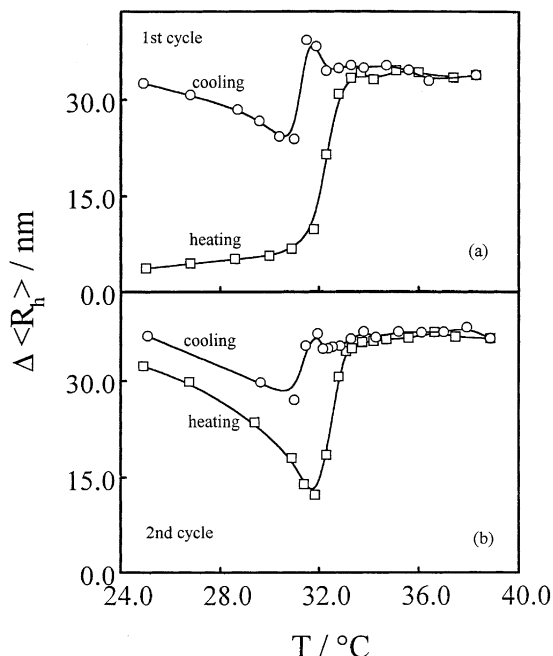


Figure 2. Temperature dependence of average thickness of the adsorbed polymer layer ($\Delta\langle R_h \rangle = \langle R_h \rangle - \langle R_{h,0} \rangle$) for the mixture of PN2 and PS22, where $\langle R_{h,0} \rangle$ and $\langle R_h \rangle$ are the average hydrodynamic radii of the particles before and after adsorption, respectively, and the PN2/PS22 macroscopic weight ratio is 2.

Before the adsorption, the weight-average molar masses ($M_{w,particle}$) of PS22 and PS60 determined by LLS were 1.48×10^7 and 3.06×10^8 g/mol, respectively. On average, each PS22 (or PS60) particle has a surface area of 6.08×10^3 (or 4.52×10^4) nm^2 . In the cooling process, most of the chains adsorbed at higher temperatures gradually escape from the particle surface because water is a good solvent for PNIPAM when $T \sim 30.5$ °C. After the first heating-and-cooling cycle, the value of the adsorption density ($\langle \sigma \rangle$) at 25 °C is higher. However, such a difference in $\langle \sigma \rangle$ was not observed in the second heating-and-cooling cycle. Therefore, the higher $\langle \sigma \rangle$ observed in the first cycle could not be attributed to the previously suggested knotting of the chains during the chain-shrinking process,²⁰ but was related to an additional adsorption.

It is known that a long PNIPAM chain in water can undergo a coil-to-globule transition when the solution is heated.⁸ It is expected that such a transition on the surface should spare more surface for additional adsorption during the heating. The total available surface limits the maximum adsorption so that $\langle \sigma \rangle$ approaches a constant at ~ 35 °C. It should be noted that each data point in Figure 1 was obtained after the temperature reached a constant value. The hysteresis in both the first and second heating-and-cooling cycles indicates the formation of an additional interchain association in the collapsed state at higher temperatures,²⁰ presumably interchain hydrogen bonding. Such an additional association could be completely destroyed only when water becomes a very good solvent at a sufficiently low temperature. This hysteresis corresponds well to the hysteresis of the melting of a single PNIPAM globule free in water.²¹

Figure 2a shows that, in the first heating process, the average hydrodynamic thickness $\Delta\langle R_h \rangle$ of the adsorbed PNIPAM layer follows a pattern similar to that of $\langle \sigma \rangle$ in Figure 1. However, $\Delta\langle R_h \rangle$ and $\langle \sigma \rangle$ behave quite differently in the first cooling process. A combination of Figures 1 and 2 leads to the following results. During the first cooling process, the desorption is accompanied by the swelling of the adsorbed chains in the range 38–31.5 °C. In the range 31.5–30.5 °C, the desorption becomes

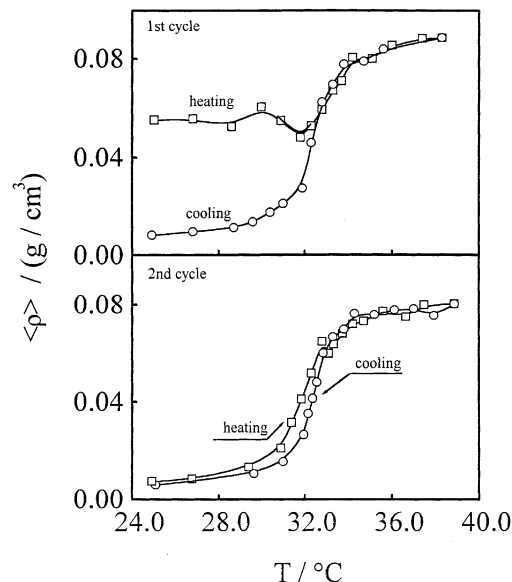


Figure 3. Temperature dependence of chain density ($\langle \rho \rangle$) of the adsorbed polymer layer for the mixture of PN2 and PS22. $\langle \rho \rangle = (M_w - M_{w,0})/V$; $M_{w,0}$ and M_w are the weight-average molar masses of the particles before and after adsorption, respectively, V is the average hydrodynamic volume of the adsorbed polymer layer, defined in the text, and the PN2/PS22 macroscopic weight ratio is 2.

so dominant that the shell thickness decreases. Finally, the desorption nearly stops, but the adsorbed chains continuously swell in the range ~ 30 – 25 °C as the temperature decreases. After the first heating-and-cooling cycle, $\langle \sigma \rangle$ at 25 °C only slightly increased, but there was a big difference in $\Delta\langle R_h \rangle$. This indicates that the adsorption of more chains on the surface forced the chains to stretch. In the second heating process, the decrease of $\Delta\langle R_h \rangle$ in the range 25–32 °C reflects the shrinking of the adsorbed chains. The following sharp increase of $\Delta\langle R_h \rangle$ was again due to additional adsorption. The adsorption was saturated at ~ 34 °C. In Figure 2, the change of $\Delta\langle R_h \rangle$ in the first and second cooling processes was similar. The little bump near ~ 31 °C in the cooling process reveals the swelling of the adsorbed chains just before the desorption started. It is helpful to note that the ratio of $\langle R_g \rangle / \langle R_h \rangle$ was always less than 0.78 predicted for a uniform hard sphere. This was because the particle with the adsorbed chains has a core-shell structure and the core has a higher density than the shell. It should be stated that no interparticle adsorption (i.e., the bridging effect) was observed because the dispersion was very dilute.

Figure 3 shows a better presentation of the adsorption in terms of the average chain density ($\langle \rho \rangle$) of the adsorbed PNIPAM layer. $\langle \rho \rangle$ reflects the packing of the chains adsorbed on the surface. In the initial stage of the first heating process, $\langle \rho \rangle$ nearly remains a constant since both $\langle \sigma \rangle$ and $\langle R_h \rangle$ only slightly increase. In the range ~ 31.5 – 35 °C, the sharp increase of $\langle \rho \rangle$ is due to the additional adsorption. In the first cooling process, both the desorption and stretching of the adsorbed chains lead to the decrease of $\langle \rho \rangle$. In Figure 3a, the difference in $\langle \rho \rangle$ at 25 °C after the first heating-and-cooling cycle clearly reveals the stretching of the chains adsorbed on the particle surface. Figure 3 reveals that, even in the collapsed state at ~ 38 °C, $\langle \rho \rangle$ is only ~ 0.1 g/cm^3 , indicating that the adsorbed polymer layer still contains $\sim 90\%$ water if we assume that bulk PNIPAM has a density of ~ 1 g/cm^3 . The PNIPAM chains on the surface collapse less than individual chains free in water.²² This is because the adsorption of a chain on the surface results in many small chain “loops” and the collapse of these small loops are more difficult due to the rigidity of the chain backbone.

TABLE 1: Heating Rate Dependence of the Adsorption of PNIPAM on Polystyrene Nanoparticles

	below LCST 31.0 °C		above LCST					
	31.0 °C		32.3 °C		33.5 °C		36.2 °C	
	slow ^a	fast ^a	slow	fast	slow	fast	slow	fast
$\Delta\langle R_h \rangle / \text{nm}$	6.90	9.00	22.4	15.8	22.8	10.3	34.7	6.6
$\sigma / (\text{mg}/\text{m}^2)$	0.47	0.78	2.64	2.19	7.87	2.14	9.93	1.81
$\rho / (\text{g}/\text{cm}^3)$	0.05	0.06	0.05	0.07	0.14	0.14	0.08	0.21

^a Slow heating rate: Heating the mixture inside the light-scattering cell holder from 25 °C to the desired temperature by a small temperature increment. After each increment, the temperature of the mixture was allowed to reach its equilibrium. Fast heating rate: Heating the LLS cell holder to the desired temperature and then transferring the mixture at 25 °C directly into the cell holder.

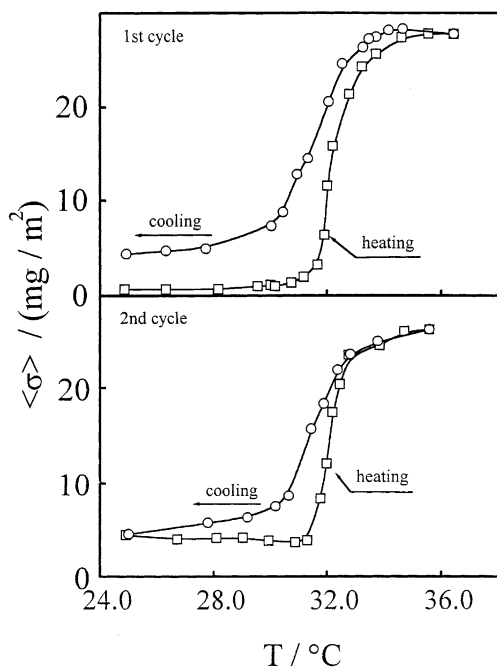


Figure 4. Temperature dependence of adsorption density ($\langle\sigma\rangle$) for the mixture of PN2 and PS60, where the PN2/PS60 macroscopic weight ratio is 2.

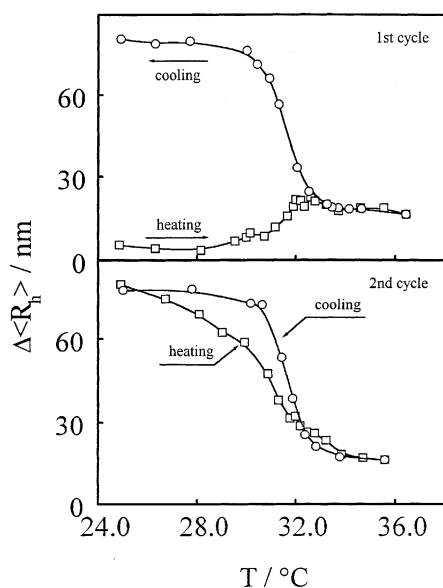


Figure 5. Temperature dependence of average thickness of the adsorbed polymer layer ($\Delta\langle R_h \rangle$) for the mixture of PN2 and PS60, where the PN2/PS60 weight ratio is 2.

Figures 4–6 are the results of a comparative study of the adsorption of PNIPAM on larger polystyrene particles ($\langle R_{h,o} \rangle = 60$ nm). It is clear that the temperature dependence of $\langle\sigma\rangle$

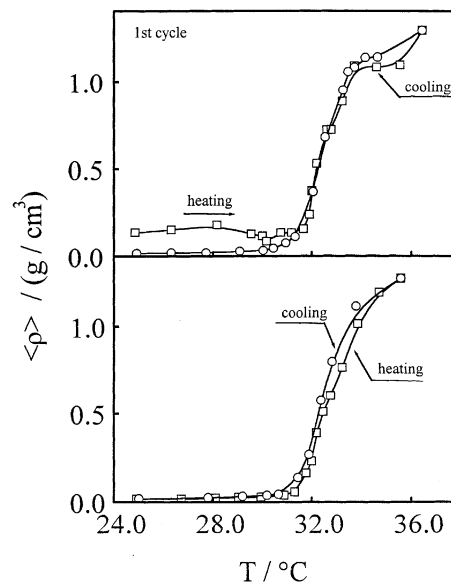


Figure 6. Temperature dependence of average density ($\langle\rho\rangle$) of the adsorbed polymer layer for the mixture of PN2 and PS60, where the PN2/PS60 weight ratio is 2.

for larger particles is similar to that in Figure 1, but $\langle\sigma\rangle$ is much higher. This is consistent with the predicted curvature effect.²³ In comparison with Figure 1, we know that adsorption is ~ 3 times higher for larger particles. Note that the total particle surface area (S) is reversibly proportional to the particle size (R) for a given latex weight concentration; i.e., $S \propto 1/R$. It agrees well since the particle size in Figure 5 is ~ 3 times larger than that in Figure 1. This clearly indicates that the total surface area available in the dispersion determines the maximum adsorption at higher temperatures. In the first heating process, the additional adsorption at higher temperature overrides the chain shrinking so that the average thickness of the adsorbed layer increases. In the second heating process, the additional adsorption is relatively lower at higher temperatures so that the chain shrinking leads to the decrease of $\Delta\langle R_h \rangle$. On the basis of the same reason, the stretching of the adsorbed chains in the second cooling process is so dominant that $\langle\sigma\rangle$ decreases but $\Delta\langle R_h \rangle$ increases. Figure 6 shows that in the collapsed state at ~ 36 °C $\langle\rho\rangle$ is slightly higher in comparison with those in Figure 3. The hysteresis at lower temperatures in the first heating-and-cooling cycle also confirms the additional adsorption. Note that in the heating process the additional adsorption only occurs after the shrinking of the chains on the particle surface. The cooling process has a lower transition temperature than the heating process because of the formation of interchain and intrachain hydrogen bonding in the collapsed state.²²

Table 1 summarizes the results of the heating rate dependence of the chain adsorption. It is clear that a fast heating of the mixture from 25 °C to a temperature higher than the LCST (~ 32 °C) results in a smaller $\Delta\langle R_h \rangle$ and a lower $\langle\sigma\rangle$. This is because

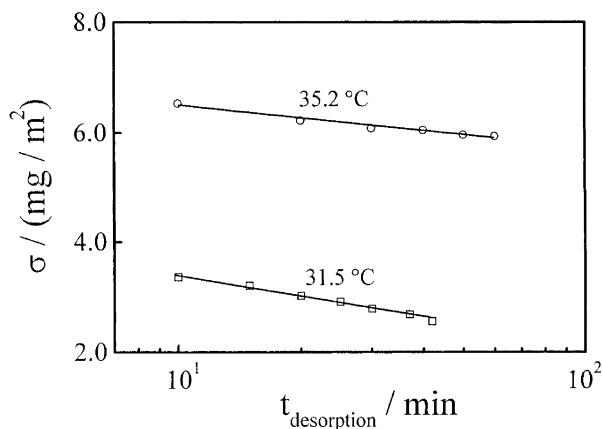


Figure 7. Desorption kinetics for the mixture of PN2 and PS22 at two temperatures, where the PN2/PS60 macroscopic weight ratio is 2.

at temperatures higher than ~ 32 °C the PNIPAM chains on the surface and in the solution collapse. In the fast heating process, on the one hand, the shrinking of the chains was so quick that the chains adsorbed on the surface have less chance to undergo interchain association to attract those chains free in solution onto the surface. On the other hand, it is expected that the adsorption of the chains collapsed into a globule form onto the surface would be more difficult than the chains swollen in the coil form due to the viscoelastic effect; namely, each collapsed chain acts as a tiny glass ball if the relaxation time of the chain inside the globule is much longer than the interaction time between the chain and the particle surface.

In contrast, heating the mixture from 25 to 31 °C leads to a much smaller $\Delta\langle R_h \rangle$ and a lower $\langle \sigma \rangle$. It is known that water at 31 °C is a slightly poor solvent and the chains are only crumpled, but not collapsed yet.⁸ The lower solubility leads to additional adsorption, resulting in the repulsion between the chains on the surface so that the chains are stretched. However, the hydrophobicity of PNIPAM at 31 °C is not so high that both $\Delta\langle R_h \rangle$ and $\langle \sigma \rangle$ are smaller. The heating rate dependence of $\langle \rho \rangle$ is more complicated because $\langle \rho \rangle$ is a function of both the adsorption and the stretching of the chains. The complicated pattern of $\langle \rho \rangle$ in Table 1 can be attributed to the competition between the collapse of the adsorbed chain and the additional adsorption.

Our results showed that the desorption of the shortest PNIPAM chains (PN1) was too fast to be observed in our present setup. This is because a short chain is not able to form a multipoint adsorption as well as a long chain. Moreover, the adsorption of several short chains is not favored in entropy in comparison with the adsorption of a long chain.²⁴ Note that in the hydrophobic adsorption there exists a dynamic equilibrium between the adsorption and desorption for each adsorbed (anchoring) point. The desorption of a long polymer chain requires not only a simultaneous release (desorption) of all the anchoring points, but also a fast diffusion of the chain away from the particle surface, which is difficult, if not impossible, for a long chain with many anchoring points attached on the surface. Therefore, we found nearly no desorption for the longest chains (PN4), so we were only able to study the adsorption and desorption of the chains with a proper length.

Figure 7 shows the desorption kinetics of the chains from the particle surface at two different temperatures. The semi-logarithmic plot of $\langle \sigma \rangle$ versus t is a straight line, revealing that the desorption is governed by diffusion.²⁵ The extrapolation of each line to $t = t_{\text{desorption}}$ represents the adsorption at each given temperature. As expected, adsorption increases with temperature, consistent with our previous results, and desorption at temper-

atures lower than the LCST (~ 32 °C) is faster than that at higher temperatures because water is a better solvent for PNIPAM at lower temperatures. The slope of each line in Figure 7 corresponds to a desorption rate.

Conclusion

In summary, our results showed that, in the hydrophobic adsorption of thermally sensitive poly(*N*-isopropylacrylamide) (PNIPAM) on the surface of surfactant-free polystyrene latex nanoparticles, there existed a hysteresis of the adsorption in the heating-and-cooling cycle, indicating an additional interchain association formed at higher temperatures, presumably hydrogen bonding. Therefore, decreasing the solvent quality can enhance the adsorption in practice. The temperature as one of the stress effects can be used to regulate the adsorption. Our results also revealed that in the cooling process the desorption and the swelling of the adsorbed chains are so correlated that they greatly affect the chain density of the adsorbed polymer layer. Moreover, we have shown that the desorption of long PNIPAM chains from the surface at lower temperatures is controlled by diffusion.

Acknowledgment. The financial support of the BASF-Sino Research & Development fund, the CAS Bai Ren Project, and the HKSAR Earmarked RGC Grants (CUHK/4266/00P, 2160135) is gratefully acknowledged.

References and Notes

- Caruso, F.; Mohwald, H. *J. Am. Chem. Soc.* **1999**, *121*, 6039.
- Oya, T.; Enoki, T.; Grosberg, A. Yu.; Masamune, S.; Sakiyama, T.; Takeoka, Y.; Tanaka, K.; Wang, G.; Yilmaz, Y.; Field, M. S.; Dasari, R.; Tanaka, T. *Science* **1999**, *286*, 1543.
- Fischer, P.; Laschewsky, A. *Macromolecules* **2000**, *33*, 1100.
- Afif, A.; Hommel, H.; Legrand, A. P.; Bacquet, M.; Gailliez-Degremont, E.; Morcellet, M. *J. Colloid Interface Sci.* **1999**, *211*, 304.
- Hu, T.; Gao, J.; Wu, C. *J. Macromol. Sci. Phys.* **2000**, *B39* (3), 407 and references therein.
- Kondo, A.; Fukuda, H. *J. Colloid Interface Sci.* **1998**, *198*, 34.
- Lee, W.-k.; McGuire, J.; Bothwell, M. K. *J. Colloid Interface Sci.* **1999**, *213*, 265.
- Schild, H. G. *Prog. Polym. Sci.* **1992**, *17*, 163 and references therein.
- Gao, J.; Wu, C. *Macromolecules* **1997**, *30*, 6873.
- Tanahashi, T.; Kawaguchi, M.; Honda, T.; Takahashi, A. *Macromolecules* **1994**, *27*, 606.
- Gao, J.; Hu, T.; Zhang, Y.; Wu, C. *Chin. J. Polym. Sci.* **1999**, *17*, 595.
- Zhulina, E. B.; Borisov, O. V.; Pryamitsyn, V. A.; Birshtein, T. M. *Macromolecules* **1991**, *24*, 140.
- Kling, J. A.; Ploehn, H. J. *J. Colloid Interface Sci.* **1998**, *198*, 241.
- Zhou, S. Q.; Fan, S. Y.; Au-yeung, S. T. F.; Wu, C. *Polymer* **1995**, *36*, 1341.
- Chu, B. *Laser Light Scattering*, 2nd ed.; Academic Press: New York, 1991.
- Berne, B.; Pecora, R. *Dynamic Light Scattering*; Plenum Press: New York, 1976.
- Wu, C.; Xia, K. Q. *Rev. Sci. Instrum.* **1994**, *65*, 587.
- Zimm, B. H. *J. Chem. Phys.* **1948**, *16*, 1099.
- Xia, J.; Dubin, P. In *Macromolecular Complexes in Chemistry and Biology*; Dubin, P., Bock, J., Davies, R. M., Schulz, D. N., Thies, C., Eds.; Springer-Verlag: New York, 1994; p 247.
- Gao, J.; Wu, C. *Chin. J. Polym. Sci.* **1999**, *17* (6), 595.
- Zhu, P. W.; Napper, D. H.; *J. Colloid Interface Sci.* **1994**, *164*, 380; *J. Colloid Interface Sci.* **1994**, *168*, 489.
- Wu, C.; Wang, X. H. *Phys. Rev. Lett.* **1998**, *79*, 4092.
- Wu, C.; Zhou, S. Q. *Phys. Rev. Lett.* **1996**, *77*, 3053.
- Biver, C.; Hariharan, R.; Mays, J.; Russel, W. B. *Macromolecules* **1997**, *30*, 1787.
- Fleer, G. J.; Cohen Stuart, M. A.; Scheutjens, J. M. H. M.; Cosgrove, T.; Vincent, B. *Polymers at Interfaces*, 1st ed.; Cambridge University Press: Cambridge, UK, 1993.